

# Toughening Effect of ZrB<sub>2</sub> in Al<sub>2</sub>O<sub>3</sub>-ZrB<sub>2</sub> Nanocomposite Ceramics

Wang Xiaomin<sup>1,2</sup>, La Peiqing<sup>1</sup>, Wang Bingjun<sup>2</sup>, Yang Guolai<sup>1</sup>

<sup>1</sup> State Key Laboratory of Advanced Processing and Recycling of Non-ferrous Metals, Lanzhou University of Technology, Lanzhou 730050, China; <sup>2</sup> Qinghai University, Xining 810016, China

**Abstract:** The Al<sub>2</sub>O<sub>3</sub>-ZrB<sub>2</sub> nanocomposite ceramics were prepared and the mechanical properties of the process parameters' effect were studied. The results show that for various applied sintering temperatures of Al<sub>2</sub>O<sub>3</sub> ceramics, a maximum Vickers hardness of 18 970 MPa and high reliability are attained at 1500 °C and at atmosphere sintering. The fracture toughness is (5.2±0.3) MPa m<sup>1/2</sup>. In addition, the sample is not well densified at the sintering temperature. Scanning electron microscopy (SEM) shows that fine ZrB<sub>2</sub> particles disperse and are pinned at grain boundaries to inhibit grain boundary movement effectively. While larger ZrB<sub>2</sub> particles distribute between Al<sub>2</sub>O<sub>3</sub> particles uniformly and occupy Al<sub>2</sub>O<sub>3</sub> particles growing space to hinder the matrix grains, which greatly promote the densification of the ceramic and improve the microstructure. 20% ZrB<sub>2</sub>/Al<sub>2</sub>O<sub>3</sub> composite ceramics exhibit a relative density above 98% at (450 °C, Vickers hardness of 18 070 MPa, and fracture toughness of (6.7±0.2) MPa m<sup>1/2</sup> Fracture morphology indicates that trans-granular fracture occurs in the nanocomposite ceramic with high toughness.

**Key words:** atmospheric sintering; nano alumina ceramic; nanocomposite ceramics; toughening

As we all know, Al<sub>2</sub>O<sub>3</sub> ceramic is a representative of the advanced ceramics industry, which has a series of advantages such as high melting point, high hardness, corrosion resistance, heat resistance and good electrical insulation properties, so it can be used in demanding conditions. Furthermore, Al<sub>2</sub>O<sub>3</sub> ceramic has become one of the important and widely used base materials in the science and technology field because of its mature production technology, production volume and low price.<sup>[1-2]</sup> Al<sub>2</sub>O<sub>3</sub> ceramic is usually applied to the structure parts to withstand mechanical stress, tool material, wear parts, bio-ceramics field, aerospace, energy, aerospace, chemical, electronics, and so on. The research of Al<sub>2</sub>O<sub>3</sub> ceramic is of great importance for science and technology workers, and it has become an extremely rapid development field in the last 20 years.<sup>[3,4]</sup> In these 20 years, the research of ZrO<sub>2</sub> particle toughening Al<sub>2</sub>O<sub>3</sub> ceramic materials is more and more, and some of the research have been applied to the practice. But in these studies, zirconia is usually used to toughen alumina, and

certain powder is required: either both nano powder<sup>[2,3,5]</sup>, or nano ZrO<sub>2</sub> powder and micron Al<sub>2</sub>O<sub>3</sub> powder with formation of "intragranular" structure after sintering<sup>[3,6]</sup>. However, the reports of ZrB<sub>2</sub> toughened alumina ceramic are few, especially the study of less-micron ZrB<sub>2</sub> toughened nano-alumina.

The present paper employs atmospheric sintering, high purity nano Al<sub>2</sub>O<sub>3</sub> powder and micron ZrB<sub>2</sub> powder to produce Al<sub>2</sub>O<sub>3</sub> ceramic and ZrB<sub>2</sub>/Al<sub>2</sub>O<sub>3</sub> composite ceramics and study the microstructure and mechanical properties.

## 1 Experiment

A kind of high purity nano-Al<sub>2</sub>O<sub>3</sub> (Shanghai, purity of 99.99%) and micron ZrB<sub>2</sub> (Lanzhou University and Technology, purity of 98%) containing a small amount of ZrO<sub>2</sub>, as shown in Fig.1 were selected as starting materials and their properties are listed in Table 1.

There is a clear difference before and after treatment of Al<sub>2</sub>O<sub>3</sub> powder. Firstly, we pre-processed a large amount of Al<sub>2</sub>O<sub>3</sub>

Received date: July 25, 2015

Foundation item: Natural Science Foundation of Qinghai Province Science and Technology Department (2012-Z-924Q); the Postdoctoral Research Fund of Lanzhou University of Technology

Corresponding author: Wang Xiaomin, Ph. D., Associate Professor, State Key Laboratory of Advanced Processing and Recycling of Non-ferrous Metals, Lanzhou University of Technology, Lanzhou 730050, P. R. China, Tel: 0086-971-5310440, E-mail: ty.com.cn@126.com

Copyright © 2016, Northwest Institute for Nonferrous Metal Research. Published by Elsevier BV. All rights reserved.

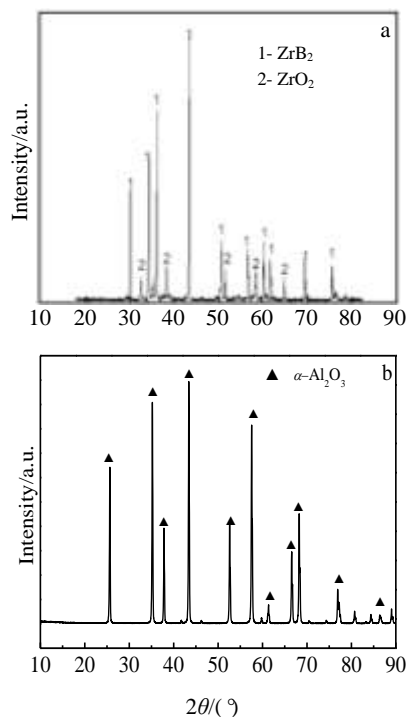


Fig.1 XRD patterns of  $\text{Al}_2\text{O}_3$  (a) and  $\text{ZrB}_2$  (b)

particles to make them get together (Fig.2a), but they dispersed after ethanol treatment, which reduced the force between the particles, so the aggregates were dispersed (Fig.2b). The grain size of  $\text{Al}_2\text{O}_3$  is about 100 nm. Fig.2c is a scanning electron micrograph of the  $\text{ZrB}_2$  powder. The individual particles are relatively large (10  $\mu\text{m}$ ), average particle size of most of other particles is about 0.3  $\mu\text{m}$  and they uniformly dispersed in the conductive adhesive.

The high-purity nano- $\text{Al}_2\text{O}_3$  powder (99.99% purity) and micron  $\text{ZrB}_2$  powder, according to the ratio shown in Table 2 were loaded into a four steel mill pot. After stirring with a spoon, corundum balls (according ball and raw material ratio is 2:1) were used to mill for 8 h on QM-2SP20-CL planetary ball mill (Nanjing University Instrument, Nanjing, China). After milling, artificial granulation was conducted. Then we let the powder through 60 mesh sieve and dried it in a thermostatic oven for 2 h and loaded a die a steel mold for dry pressing at 450 MPa with Guo-long four-column universal hydraulic machine of Nantong China. After forming, the sample was a cylinder with size  $\Phi 25 \text{ mm} \times 7 \text{ mm}$  (named as green). Then we put the green into the TC-17X sintering furnace whose heating source was composed of 24  $\text{MoSi}_2$  rods

(bar) atmospheric sintering at 1500  $^\circ\text{C}$  or 1450  $^\circ\text{C}$ , heating rate is 15  $^\circ\text{C}/\text{min}$ . The sintering system is shown in Fig.3.

The sintered ceramic material samples were ground and polished with sandpaper 600, 800, 1000, 1200, 1500 and 2000 mesh. Vickers hardness was measured with MVC-1000JMT1 micro Vickers hardness tester with load of 200 gf, holding time of 15 s, equipped with 400 optical microscope. The phase composition of the sintered composite materials or the raw materials was analyzed by X-ray diffraction (XRD) (D8ADVANCE X-ray diffraction, Rigaku Company). Material microstructure morphology, polished surface and fracture morphology of the sample were detected by JSM-6700F field emission scanning electron microscope (FESEM, JEOL Company, Japan).

## 2 Results and Discussion

### 2.1 Sintering system

Fig.4 and Fig.5 shows the Vickers hardness and relative density of materials at different temperatures, respectively. At 1500  $^\circ\text{C}$ , the  $\text{Al}_2\text{O}_3$  ceramic's Vickers hardness is 18 970 MPa, and it almost remains the value. But, the  $\text{ZrB}_2\text{-Al}_2\text{O}_3$  ceramic's Vickers hardness is 18 070 MPa, which is lower than  $\text{Al}_2\text{O}_3$  ceramic's, and also almost remains the level. At 1400  $^\circ\text{C}$ , the relative density of both ceramics is more than 99%. Therefore, the two samples, sample A of pure  $\text{Al}_2\text{O}_3$  sintered at 1500  $^\circ\text{C}$ , and sample B of  $\text{ZrB}_2$  (20wt%) +  $\text{Al}_2\text{O}_3$  (80 wt%) sintered at 1450  $^\circ\text{C}$ , were selected to determine the properties of toughened.

### 2.2 Phase composition and microstructure of $\text{Al}_2\text{O}_3$ ceramics

SEM image of the sample A is shown in Fig.6a. We can see obviously that its quality is not very good, mainly because the sintering temperature is not enough to completely form porcelain, and the grain size is 200~300 nm. When the purity of  $\text{Al}_2\text{O}_3$  increases, and the sintering temperature increases too, grains grow rapidly. It can be seen from the fracture surface topography in Fig.6b that the fracture mode is obvious intergranular fracture.

### 2.3 Phase composition and microstructure of $\text{ZrB}_2\text{-Al}_2\text{O}_3$ composites

Since the sintering quality of sample A is not very good, we adjusted the sintering temperature and added the second phase of  $\text{ZrB}_2$  particles to obtain good microstructural and mechanical properties.  $\text{ZrB}_2$  particle dispersion can toughen the material. From the XRD patterns (Fig.7) of sample B shows that the phase transformation toughening phenomenon

Table 1 Starting materials properties

Starting materials	Density/g $\text{cm}^{-3}$	Thermal expansion coefficient/ $\times 10^{-6} \text{ K}^{-1}$	Poisson's ratio	Modulus of elasticity/GPa	Grain size	Purity/%
$\text{Al}_2\text{O}_3$	3.98	8.4	0.26	400	<200 nm	99.99
$\text{ZrB}_2$	6.085	5.9	0.2422	387	0.1~10 $\mu\text{m}$	99

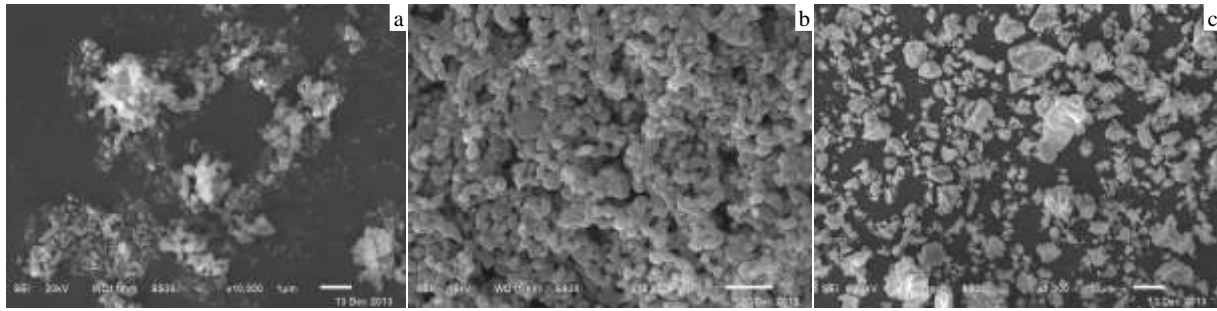


Fig.2 Starting materials' SEM images: (a)  $\alpha$ -Al<sub>2</sub>O<sub>3</sub> before treating, (b)  $\alpha$ -Al<sub>2</sub>O<sub>3</sub> after treating and (c) ZrB<sub>2</sub>

Table 2 Experimental ratio and sintering parameters

Samples	Composition, $\phi$ /%		Sintering parameters		
	Al <sub>2</sub> O <sub>3</sub>	ZrB <sub>2</sub>	Sintering temperature/ °C	Molding pressure/MPa	Insulation time/h
A	100	0	1500	450	8
B	80	20	1450	450	8

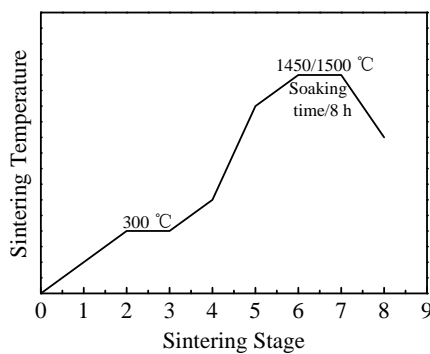


Fig.3 Curve of atmospheric sintering system

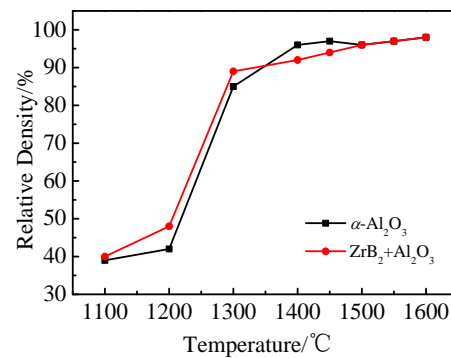


Fig.5 Relative density of materials at different sintering temperatures

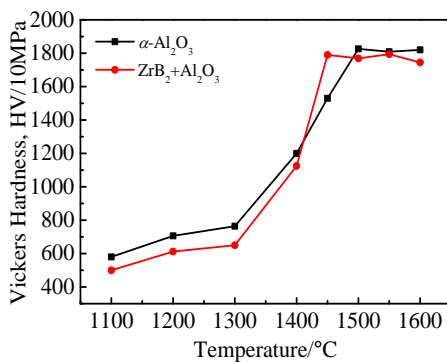


Fig.4 Vickers hardness of materials at different sintering temperatures

does not exist. The main reason of particles toughening is second phase particles of high elastic modulus added in the ceramic matrix. The thermal expansion coefficient and elastic modulus of the second phase and the matrix are mismatched, so when the fracture stress increases, the part of the fracture

energy is absorbed. The absorbed fracture energy has the dual effect of strengthening and toughening.

Fig.7a is XRD patterns of Sample B. ZrB<sub>2</sub> phase and  $\alpha$ -Al<sub>2</sub>O<sub>3</sub> phase can be seen in the composite materials, but the phase transformation toughening phenomenon does not occur, which is a great pity for toughening. Fig. 7b can explain the better performance of the materials when the micron ZrB<sub>2</sub> particles are added into the nano Al<sub>2</sub>O<sub>3</sub> matrix. Micron ZrB<sub>2</sub> particles are not spherical, but the polygonal block. These particles uniformly distribute in the matrix. Fig.8a is the surface scanning electron micrograph of the sample B. We can see that the crystal particles are uniform and spherical. The grain size is only about 100 nm, smaller than that of the pure Al<sub>2</sub>O<sub>3</sub><sup>[1,5]</sup> ceramic. Although the ZrB<sub>2</sub> particles are irregular in shape and size, they are still very uniformly distribute in the matrix. Fig.8b is a scanning electron micrograph of the fracture of sample B, in which the uniform grain size and dense microstructure can be seen clearly in the SEM. As a result, ZrB<sub>2</sub> particle size and dispersion degree, have a

significant effect on the sintering and fracture of ceramic samples: (1) the small size of the  $ZrB_2$  pinned on the  $Al_2O_3$  grain boundaries which inhibits the growth of the matrix grains<sup>[7-9]</sup> (Fig.8c, the arrows show the pinning phenomenon). (2) the large particle size  $ZrB_2$  effectively suppresses matrix grain growth, and block and disperse the crack, increases the expansion path and consume more fracture energy. In Fig.8d as indicated by the arrows, the transgranular fracture occurs on the large particles. This is because the tiny  $ZrB_2$  particles

are pinned grain boundaries and make the intergranular combination very strong, forcing the crack propagation along the cleavage plane of the larger particles, and the transgranular fracture occurs. Its appearance will absorb part of the energy at break, and extremely favorable for improving the fracture toughness. The fracture mode is a mixed fracture mode with intergranular fracture as the main mode (Fig.8b).

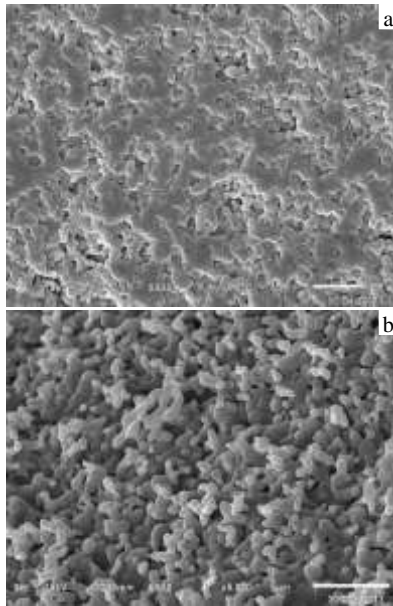


Fig.6 SEM image (a) and fracture morphology (b) of sample A (pure  $Al_2O_3$ , 1500 °C, 8 h)

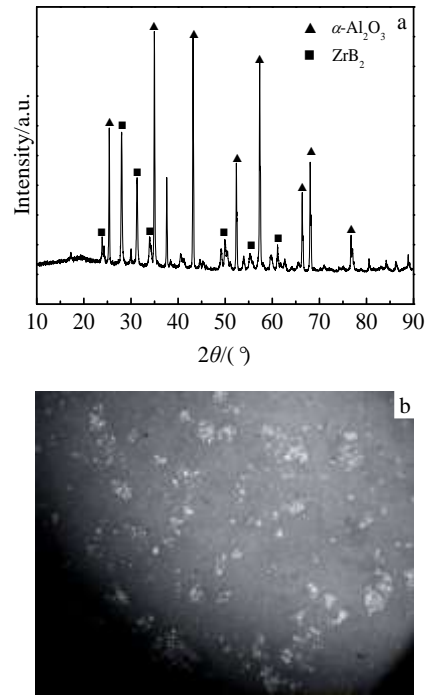


Fig.7 XRD pattern (a) and photomicrograph (b) of sample B

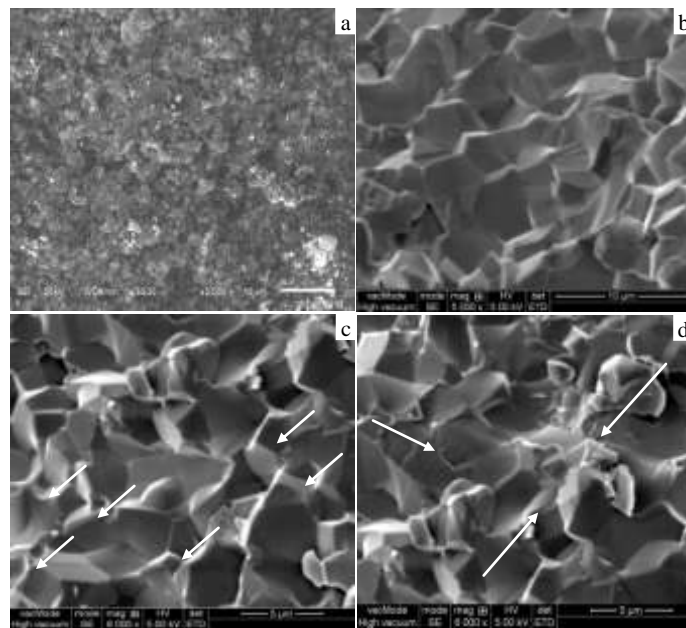


Fig.8 SEM image (a) and fracture morphologies (b, c, d) of sample B (1450 °C, 8 h)

## 2.4 Ceramic toughness calculation

The toughness of the ceramics were measured and calculated by Laugier II (DCM8)<sup>[10,11]</sup> formula:

$$K_{Ic} = 0.015(L/a)^{\frac{1}{2}}(E/H)^{\frac{2}{3}} \quad (1)$$

$$PC^{-\frac{3}{2}}L/a < 2.5 \quad (2)$$

where,  $H$ : hardness of the materials;  $E$ : Elastic modulus of the material;  $P$ : Indentation, carry burden;  $L$ : Indentation crack length;  $a$ : Indentation radius;  $C=L+a$

According to the formula, the toughness of pure alumina ceramics is  $(5.2 \pm 0.3)$  MPa  $m^{1/2}$ , lower than  $(6.7 \pm 0.2)$  MPa  $m^{1/2}$  of the  $ZrB_2+Al_2O_3$  ceramics. The results indicate that the preceding analysis of  $ZrB_2$  nail toughening effect is correct.

## 3 Conclusions

1) Pure  $Al_2O_3$  ceramic's microstructure is poor when atmospheric sintering and its fracture morphology is intergranular fracture. The  $Al_2O_3$  ceramic has a Vickers hardness of 18 970 MPa and the fracture toughness of  $(5.2 \pm 0.3)$  MPa  $m^{1/2}$  when sintered above 1500 °C. Correspondingly, the  $ZrB_2-Al_2O_3$  ceramic has a Vickers hardness of 18 070 MPa and the fracture toughness of  $(6.7 \pm 0.2)$  MPa  $m^{1/2}$  when sintered above 1450 °C.

2) The microstructure of  $ZrB_2+Al_2O_3$  is good.  $ZrB_2$  with small grain size is distributed in the  $Al_2O_3$  matrix uniformly,

playing the role of pinning. However, larger particles block and disperse the crack, so the fracture toughness and microstructure are improved.

3) Fracture morphology of  $ZrB_2+Al_2O_3$  indicates that intergranular fracture is the main way of mixed fracture mode.

## References

- 1 Rao Pinggen, Iwasa Mikio, Kondoh Isao. *J Mater Sci Lett*[J], 2000, 19(7): 543
- 2 Ma Weimin, Wen Lei, Guan Renguo et al. *Materials Science and Engineering A*[J], 2008, 477(1): 100
- 3 Zu Yufei, Chen Guoqing, Fu Xuesong et al. *Ceramics International*[J], 2014, 40(3): 3989
- 4 Dillon S J, Harmer M P. *J Eur Ceram Soc*[J], 2008, 28(7): 1485
- 5 Lee B T, Sarkar S K, Song H Y. *J Eur Ceram Soc*[J], 2008, 28(1): 229
- 6 Voytovych R, MacLaren I, Gülgün M A et al. *Acta Mater*[J], 2002, 50(13): 3453
- 7 Fang J, Thompson A M, Harmer M P et al. *J Am Ceram Soc*[J], 1997, 80(8): 2005
- 8 Dillon S J, Harmer M P. *Acta Materialia*[J], 2007, 55(15): 5247
- 9 Dillon S J, Harmer M P, Rohrer G S. *Acta Materialia*[J], 2010, 58(15): 5097
- 10 Lawn B R, Evans A G, Marshall D B. *J Amer Ceram Soc*[J], 1980, 63(9-10): 574
- 11 Wang Zongying, Li Li, Inga-Lill Ekberg. *J Shenyang Archit Civil Eng Univ: Nat Sci*[J], 1991, 7(4): 403 (in Chinese)

## ZrB<sub>2</sub> 在 Al<sub>2</sub>O<sub>3</sub>-ZrB<sub>2</sub> 复相陶瓷中的增韧性能

王晓民<sup>1,2</sup>, 喇培清<sup>1</sup>, 王丙军<sup>2</sup>, 杨国来<sup>1</sup>

(1. 兰州理工大学 省部共建有色金属先进加工与再利用国家重点实验室, 甘肃 兰州 730050)

(2. 青海大学, 青海 西宁 810016)

**摘要:** 常压烧结制备了  $Al_2O_3$  和 20% $ZrB_2/Al_2O_3$  (质量分数)复合陶瓷, 用 XRD 和金相显微镜、SEM 分析了其相组成、微观结构、断裂形貌, 并用压痕法计算了陶瓷的断裂韧性。结果表明:  $Al_2O_3$  陶瓷自 1500 °C 开始其相对密度超过 99%, 维氏硬度达到 18 970 MPa, 断裂韧性为  $(5.2 \pm 0.3)$  MPa  $m^{1/2}$ ; 20% $ZrB_2/Al_2O_3$  复合陶瓷在 1450 °C 时相对密度超过 98%, 维氏硬度达到 18 070 MPa, 断裂韧性为  $(6.7 \pm 0.2)$  MPa  $m^{1/2}$ 。微观形貌观察表明,  $ZrB_2/Al_2O_3$  复合陶瓷韧性的增加是由于弥散分布的  $ZrB_2$  在  $Al_2O_3$  陶瓷基体中起到遏制裂纹扩展和钉扎双重作用的结果。

**关键词:** 常压烧结; 纳米氧化铝陶瓷; 纳米复相陶瓷; 增韧

作者简介: 王晓民, 男, 1975 年生, 博士, 副教授, 兰州理工大学省部共建有色金属先进加工与再利用国家重点实验室, 甘肃 兰州 730050, 电话: 0971-5310440, E-mail: ty.com.cn@126.com